Modeling of Pharmaceutical Biotransformation by Enriched Nitrifying Culture under Different Metabolic Conditions

Xu, Yifeng; Chen, Xueming; Yuan, Zhiguo; Ni, Bing-Jie

Published in:
Environmental Science & Technology

Link to article, DOI:
10.1021/acs.est.8b00705

Publication date:
2018

Document Version
Peer reviewed version

Article

Modeling of Pharmaceutical Biotransformation by Enriched Nitrifying Culture under Different Metabolic Conditions

Yifeng Xu, Xueming Chen, Zhiguo Yuan, and Bing-Jie Ni

Environ. Sci. Technol., **Just Accepted Manuscript** • DOI: 10.1021/acs.est.8b00705 • Publication Date (Web): 15 Feb 2018

Modeling of Pharmaceutical Biotransformation by Enriched Nitrifying Culture under Different Metabolic Conditions

Yifeng Xu[1], Xueming Chen[1,2], Zhiguo Yuan[1], Bing-Jie Ni[1,*]

[1]Advanced Water Management Centre, The University of Queensland, St. Lucia, Brisbane, QLD 4072, Australia

[2]Process and Systems Engineering Center (PROSYS), Department of Chemical and Biochemical Engineering, Technical University of Denmark, 2800 Kgs. Lyngby, Denmark

***Corresponding author:**

Phone: + 61 7 3346 3219; Fax: +61 7 3365 4726; E-mail: bingjieni@gmail.com

Table of Contents (TOC) Art

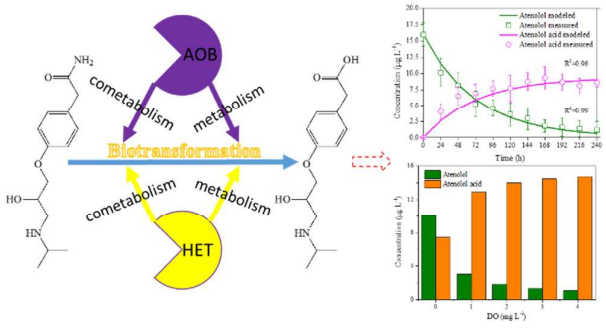

Abstract

Pharmaceutical removal could be significantly enhanced through cometabolism during nitrification processes. So far pharmaceutical biotransformation models have not considered the formation of transformation products associated with the metabolic type of microorganisms. Here we reported a comprehensive model to describe and evaluate the biodegradation of pharmaceuticals and the formation of their biotransformation products by enriched nitrifying cultures. The biotransformation of parent compounds was linked to the microbial processes via cometabolism induced by ammonium oxidizing bacteria (AOB) growth, metabolism by AOB, cometabolism by heterotrophs (HET) growth and metabolism by HET in the model framework. The model was calibrated and validated using experimental data from pharmaceuticals biodegradation experiments at realistic levels, taking two pharmaceuticals as examples, i.e., atenolol and acyclovir. Results demonstrated the good prediction performance of the established biotransformation model under different metabolic conditions, as well as the reliability of the established model in predicting different pharmaceuticals biotransformations. The linear positive correlation between ammonia oxidation rate and pharmaceutical degradation rate confirmed the major role of cometabolism induced by AOB in the pharmaceutical removal. Dissolved oxygen was also revealed to be capable of regulating the pharmaceutical biotransformation cometabolically and the substrate competition between ammonium and pharmaceuticals existed especially at high ammonium concentrations.

Keywords: Cometabolism, pharmaceutical, model, ammonia oxidizing bacteria, biotransformation product, substrate competition

Introduction

The ubiquitous occurrence and fate of pharmaceuticals in the environment and engineering systems have attracted the concerns of the scientists and the public for decades due to their potential ecotoxic impact on aquatic ecosystems.[1,2] These organic compounds were present in the wastewater at concentrations ranging from pg L^{-1} to μg L^{-1}.[3,4] As the wastewater treatment plants (WWTPs) were originally designed for chemical oxygen demand and other nutrients removal, the incomplete removal was found for pharmaceuticals in the treatment processes, being a major pathway for pharmaceuticals to enter the environment.[5]

Autotrophic biomass (e.g., enriched nitrifying sludge) was capable of transforming the pharmaceuticals cometabolically during the wastewater treatment process and thus the pharmaceutical removal was reported to be positively correlated to nitrification rate.[6,7] Ammonia oxidizing bacteria (AOB) in the nitrifying biomass could degrade a broad range of substrates including aromatic and aliphatic compounds due to the non-specific enzyme ammonia monooxygenase (AMO).[8-10] The presence of the growth substrate (i.e. ammonium) was required for cometabolism which should be taken into account when predicting the fate of pharmaceuticals.[11] In addition to cometabolism, pharmaceuticals could also be degraded as the energy and carbon source for microorganisms through metabolic biotransformation.[11] Furthermore, the formed biotransformation products might be more toxic and persistent.[12] Hence the biotransformation products should be considered for a more comprehensive understanding of the fate of pharmaceuticals in the nitrifying activated sludge.

Mathematical modeling offers a useful tool and is adopted widely to analyze complicated metabolic pathways. Cometabolic biotransformations were previously modeled through first-order kinetics and mixed order kinetics like Monod expression[13-15] and have evolved from only considering the cometabolic substrates to incorporating the relationships between cometabolic substrates and growth substrates, such as competitive interaction and toxicity

inhibition.[15] However, the previous literature has rarely considered the formation of biotransformation products in the cometabolic biotransformation models for pharmaceuticals.

The aim of this work is to develop and test a comprehensive modeling framework to describe the pharmaceuticals biotransformation at realistic levels as well as the formation of their biotransformation products by the enriched nitrifying sludge under different metabolic conditions. Microbial processes contributing to the pharmaceutical biotransformation were considered as follows: growth-linked cometabolism by AOB, metabolic transformation by AOB, growth-linked cometabolism by heterotrophs (HET) and metabolic transformation by HET. To this end, atenolol and acyclovir were selected as the model compounds in this study as they were frequently found in the wastewater with the highest concentrations of 25 and 1.8 μg L^{-1}, respectively, which have been reported to be increasingly removed under nitrifying conditions.[16-18] It has been reported that they can be biotransformed into atenolol acid and carboxy-acyclovir, respectively.[18,19] Model calibration and validation were carried out with experimental data using atenolol as parent compounds under different metabolic conditions. Model evaluation was also conducted using the experimental data from acyclovir biotransformation. The effects of dissolved oxygen (DO) and ammonium concentrations on pharmaceutical biotransformation were investigated using the validated model to provide insights into the process dynamics. The reported model in this work is expected to be used as a tool to fully understand the fate of pharmaceuticals associated with different metabolisms by responsible microorganisms in the complicated activated sludge system.

Materials and Methods

Model development

A multi-species and multi-substrate model was developed to describe the pharmaceutical biotransformation processes by the enriched nitrifying sludge. This biotransformation model comprehensively considered the consumption of the pharmaceuticals and the formation of transformation products accompanied with the simultaneous nitrification in the enriched nitrifying sludge. It describes the relationships among eight soluble substrates as defined in Table S1 in Supporting Information (SI), i.e., ammonium (S_{NH_4}), nitrite (S_{NO_2}), nitrate (S_{NO_3}), readily biodegradable substrates (S_S), oxygen (S_{O_2}), pharmaceutical (parent compound, PC, S_{PC}), primary biotransformation product (BP, S_{BP}) and other biotransformation products (OP, S_{OP}), and five particulate species, i.e., AOB (X_{AOB}), HET (X_{HET}), NOB (nitrite oxidizing bacteria, X_{NOB}), slowly biodegradable substrates (X_S) and inert biomass (X_I). Nine processes are considered: (1) metabolic transformation of PC by AOB; (2) cometabolic transformation of PC coupled to growth of AOB; (3) endogenous decay of AOB; (4) hydrolysis; (5) metabolic transformation of PC by HET; (6) cometabolic transformation of PC coupled to growth of HET; (7) endogenous decay of HET; (8) growth of NOB; and (9) endogenous decay of NOB. The kinetic expressions and the stoichiometric matrix of the proposed biotransformation model are summarized in Tables S2 and S3 in SI, respectively. The definitions, values, units and sources of all parameters used in the biotransformation model are listed in Table S4 in SI.

Pharmaceutical biodegradation was reported to be linked to AOB due to the non-specific enzyme AMO as well as HET, which was not related to the activity of NOB.[20] In this model, the microbial growth-linked kinetic expressions (processes 2 and 6 in Table S2 in SI) are described using the Monod equations, which are associated with cometabolic biotransformation of pharmaceuticals.[20] The concentration of growth substrates S_{NH_4} and S_S is also involved in the Monod equations. The basis of the cometabolic biotransformation expressions is the concept of transformation coefficient parameters such as AOB growth-

linked $T^{c}_{PC\text{-}AOB}$ and HET growth-linked $T^{c}_{PC\text{-}HET}$. The pharmaceutical biotransformation reactions directly conducted via metabolism by AOB and HET are described by pseudo-first order kinetic expressions (processes 1 and 5 in Table S2 in SI). For each reaction, the rate is expressed by an explicit function of the concentrations of relevant pharmaceuticals in the process. For microbial metabolic biodegradation of PC, the key parameters are biomass normalized PC degradation rate coefficients in the absence of AOB and HET growth, i.e. $k_{PC\text{-}AOB}$ and $k_{PC\text{-}HET}$. Processes 1, 2, 5 and 6 together contribute to pharmaceutical biotransformation in the enriched nitrifying sludge.

The formation of biotransformation products is modeled using the specific stoichiometry coefficients in processes 1, 2, 5 and 6. The coefficients α^{m}_{BP} and α^{c}_{BP} indicate the transformation of PC to BP under metabolism and cometabolism conditions by AOB, respectively. Similarly, the coefficients β^{m}_{BP} and β^{c}_{BP} present the transformation of PC to BP under metabolism and cometabolism conditions by HET, respectively.

Atenolol and acyclovir biotransformation experiments

Experimental data from our previous biodegradation experiments of atenolol (Case *I*) and acyclovir (Case *II*) under different conditions by an enriched nitrifying sludge were used for model evaluation in this work.[21,22] The chemicals used in the batch experiments and the enrichment of nitrifying cultures in the sequencing batch reactor (SBR) are described in Text S1 and S2 in SI. Details of the experimental conditions applied in different scenarios are provided in Table S5 in SI. Briefly, 4-L beaker was used as the batch reactor with enriched nitrifying cultures inoculated to degrade parent compounds at an initial 15 μg L^{-1}. The mixed liquid suspended solid (MLVSS) concentration was kept at approximately 1 g L^{-1}. All the batch experiments were conducted in duplicates. The designs for Experiments 1-3 were same for atenolol (Case *I*) and acyclovir (Case *II*). In Experiment 1, 30 mg L^{-1} allylthiourea (ATU)

141 was added to inhibit nitrifying activities,[20,23,24] leading to the dominant contribution from
142 HET to pharmaceutical biotransformation.[11] Initial ammonium concentration was provided at
143 50 mg-N L^{-1}. No external ammonium was supplied during the entire experimental period
144 (240 h). In Experiment 2, no initial and external ammonium was provided during 240 h. In
145 Experiment 3, constant ammonium concentration was maintained at 50 mg-N L^{-1} by dosing a
146 mixture of ammonium bicarbonate and potassium bicarbonate as ammonium feeding solution
147 and pH buffer at the same time, which could ensure the cometabolic biotransformation by
148 AOB. The Experiment 4 was exclusively designed for atenolol biotransformation, where
149 constant ammonium concentrations of 25 mg-N L^{-1} were provided using the dosing method
150 in Experiment 3 during the experimental period. Samples were collected periodically to
151 analyse mixed liquid suspended solid (MLSS) concentration and its volatile fraction (i.e.,
152 MLVSS), NH_4^+, NO_2^-, NO_3^-, atenolol, acyclovir and their biotransformation products
153 atenolol acid and carboxy-acyclovir. The detailed chemical analysis procedures could be
154 found in the previous work.[21,22,25]

155 The contribution of sorption to removal of atenolol and acyclovir was insignificant based
156 on our previous studies.[22,25] This is in consistent with low sorption coefficient K_D (0.04) of
157 atenolol and low octanol-water partition coefficient Log K_{OW} (0.16) of atenolol as well as Log
158 K_{OW} (-1.59) of acyclovir.[26-28] Volatilization was considered negligible given the low values of
159 Henry's law constants for atenolol (1.37×10^{-18} atm m^3 mol^{-1}) and acyclovir (3.2×10^{-22} atm m^3
160 mol^{-1}).[29] Hydrolysis would not contribute to the degradation of atenolol and acyclovir, which
161 was confirmed previously and was in consistent with the absence of their transformation
162 products.[22,25] Photodegradation was also insignificant considering the turbidity of the sludge
163 and the aluminum foil covering the reactor. Therefore, microbially induced biodegradation
164 should be the main mechanism for pharmaceutical removal in both atenolol and acyclovir
165 biotransformation experiments.

166

167 **Model calibration and validation**

168 The biotransformation model used in this work consists of 9 biochemical processes and
169 27 stoichiometric and kinetic parameters (as shown in Tables S2 and S4 in SI). Most of these
170 parameters were well established in previous literature, therefore the reported values were
171 directly used in this developed model. However, the information on biomass growth-linked
172 PC transformation coefficients $T^c_{PC\text{-}AOB}$ and $T^c_{PC\text{-}HET}$ and microbial endogenous
173 transformation coefficients $k_{PC\text{-}AOB}$ and $k_{PC\text{-}HET}$ was limited.[20] Considering the key role of
174 cometabolism induced by AOB growth in biotransformation, the maximum specific growth
175 rate of AOB $\mu_{max,\ AOB}$ was of significance to the developed model. Furthermore, the
176 sensitivity analysis suggested the four key parameters $k_{PC\text{-}AOB}$, $k_{PC\text{-}HET}$, $T^c_{PC\text{-}AOB}$and $\mu_{max,\ AOB}$
177 are highly sensitive to the biotransformation processes in terms of the experimental
178 measurements (examples shown in Figure S1 in SI). Model calibration was therefore
179 conducted to estimate the values of $k_{PC\text{-}AOB}$, $k_{PC\text{-}HET}$, $T^c_{PC\text{-}AOB}$ and $\mu_{max,\ AOB}$ based on
180 experimental measurements through minimizing the sum of squares of the deviations
181 between the measured and modeled values for the concentrations of parent compounds and
182 biotransformation products under different conditions. In addition, the four stoichiometric
183 coefficients, i.e., α^m_{BP}, α^c_{BP}, β^m_{BP} and β^c_{BP}, for the transformation of PC to BP under metabolism
184 and cometabolism conditions could be determined based on the respective molecular mass
185 and concentrations of BP and PC measured in the experiments.

186 Experimental data from atenolol biotransformation (Case *I*) of Experiments 1-3 were
187 firstly used for model calibration. Concentrations of ammonium, nitrite, DO, atenolol and
188 atenolol acid from Experiment 1 and Experiment 2 were fitted by model simulations to
189 estimate $k_{PC\text{-}HET}$ and$k_{PC\text{-}AOB}$, respectively, whereas concentrations of ammonium, nitrite, DO,

atenolol and atenolol acid from Experiment 3 were fitted to estimate $\mu_{max,\ AOB}$ and $T^{c}_{PC\text{-}AOB}$, using the $k_{PC\text{-}HET}$ and $k_{PC\text{-}AOB}$ values obtained in previous experiments (Experiment 1 and Experiment 2). Model validation was then carried out with the calibrated parameters using the independent experimental data sets from atenolol biotransformation of Experiment 4.[21] Specifically, in Experiment 4, batch experiments with atenolol as the parent compound at an initial concentration of 15 μg L^{-1} were conducted using the same enriched nitrifying sludge (i.e., same microbial composition) in the constant presence of ammonium of 25 mg-N L^{-1} and at DO of around 2.5 mg L^{-1}. There were no significant gaps between batch experiments, leading to insignificant biomass changes. The ammonium and DO concentrations applied were different from of Experiment 3 at ammonium of 50 mg-N L^{-1} and DO of 3.0 mg L^{-1} (Table S5 in SI). To further verify the validity and applicability of the model, the model was also applied to evaluating the acyclovir biotransformation data from Case *II* of Experiments 1-3. The key model parameters were recalibrated for Case *II* using the three sets of batch experimental data (Table S5 in SI).

The sensitivity analysis, parameter estimation, parameter uncertainty evaluation and model simulations were done through employing a modified version of software AQUASIM 2.1d according to Batstone et al.[30], with a 95% confidence level for significance testing and parameter uncertainty analysis. The standard errors and 95% confidence intervals of individual parameter estimates were calculated from the mean square fitting errors and the sensitivity of the model to the parameters. Residual sum of squares (RSS) between the objective data and model was used as the objective function.

Results

Model calibration with experimental data from atenolol biotransformation

As atenolol acid was the sole biotransformation products with no other products identified in all batch experiments, the dynamics of the substrate S_{OP} was not modeled herein. The model was first calibrated to illustrate the biotransformation of atenolol catalysed solely by HET in Experiment 1 (i.e. with addition of ATU to inhibit the nitrifying activity). Given that no exogenous organic carbon was supplied during culture enrichment and the only organic carbon in the batch experiments was pharmaceuticals, the growth of HET was considered extremely low and the cometabolic transformation rate of pharmaecuticals linked to growth of HET was not modeled with $T^{c}_{PC\text{-}HET}$ omitted for estimation.[20] With AOB related parameters $k_{PC\text{-}AOB}$ and $T^{c}_{PC\text{-}AOB}$ set to zero, only the parameter k_{PC-HET} was estimated with its best-fit value shown in Table 1 for Experiment 1. The predicted atenolol and atenolol acid concentration profiles with the established model were demonstrated in Figure 1A, along with the measured experimental values. Atenolol experienced a continuous decrease by 94.3% from the beginning to the end of experiments accompanied with a gradual increase of atenolol acid until 168 h and a stable stage until 240 h at a conversion efficiency of 62.6% (Figure 1A), which was well captured by the model predictions.

The experimental data obtained from Experiment 2 (i.e., in the absence of ammonium) were used to further calibrate the developed model in terms of atenolol and atenolol acid dynamics. Without the presence of the growth substrate, the ammonium released from cell lysis process during bacterial decay was minor and AOB growth-linked cometabolism would be considered to have negligible contribution to atenolol biotransformation. Therefore, only the metabolic biotransformation by AOB and HET were involved in the biotransformation of atenolol for Experiment 2. The parameter value of $k_{PC\text{-}HET}$ obtained in Experiment 1 was used directly without any modification. Another key model parameter $k_{PC\text{-}AOB}$ related to AOB metabolism was thus reliably estimated during atenolol biotransformation (value as shown in Table 1). As shown in Figure 1B, although atenolol demonstrated a sharp decrease by 97.4%

240 over the whole experimental period, the production of atenolol acid indicated a lower
241 transformation efficiency in the absence of ammonium (29.1%) compared with the
242 experiments with addition of ATU (see Figure 1A), again well matching the model
243 predictions.

244 In Experiment 3, the presence of ammonium at 50 mg-N L^{-1} was provided constantly to
245 ensure the cometabolic biodegradation of atenolol by both AOB and HET at DO of 3.0 mg L^{-1}
246 . Together with the rest of the parameters involved, the parameter values of $k_{PC\text{-}HET}$ and
247 $k_{PC\text{-}AOB}$ estimated in the previous two experiments were applied in the biotransformation
248 model. The key parameters related to AOB induced cometabolism, i.e., $T^{c}_{PC\text{-}AOB}$ and $\mu_{max,\ AOB}$,
249 were then estimated with the optimum values listed in Table 1. Figure S2A in SI showed the
250 well agreement between predicted and measured concentrations of ammonium, nitrite and
251 DO based on the proposed model, supporting the capability of the model to describe the two-
252 step nitrification processes in terms of nitrite accumulation, as well as the suitability of the
253 selected parameters related to DO dynamics for the cometabolic biodegradation processes by
254 the enriched nitrifying culture (i.e., the $K_{O_2,AOB}$ and $K_{O_2,HET}$ values for AOB and HET). It
255 should be noted that the nitrate concentrations were not specifically modeled, which were
256 slightly higher than that in the SBR in all experiments since the biomass in batch experiments
257 was taken directly from SBR with a background nitrate concentration up to 1000 mg L^{-1}. As
258 shown in Figure 1C, concomitant with the gradual decrease of atenolol at a removal
259 efficiency of 88.0%, atenolol acid was formed at an increasing trend with 86.9% conversion
260 efficiency. This was obviously higher than the experiments in the absence of ammonium and
261 with the addition of ATU, indicating a positive role of AOB induced cometabolism in
262 atenolol transformation. The model described these observations reasonably well.

263 Overall, the developed model could satisfactorily capture all dynamics associated with
264 atenolol and atenolol acid in all batch biodegradation experiments under different metabolic

conditions. The good agreement between model simulations and measured data in Figure 1 supports the capability of the developed model in describing the microbial growth related biotransformation of atenolol in enriched nitrifying cultures. The obtained parameter linked to AOB growth during ammonia oxidation, i.e., AOB-induced cometabolic atenolol transformation coefficient $T^{c}_{PC\text{-}AOB}$, was estimated at 0.012 ± 0.000036 m^3 g COD^{-1}. It was lower than the reported value of 0.0715 ± 0.0227 m^3 g COD^{-1} for atenolol biodegradation by an enriched nitrifying sludge.[20] The non-growth metabolism by HET and the non-growth metabolism by AOB on atenolol biodegradation also described the experimental data with the addition of ATU and in the absence of ammonium well. The estimated parameters of $k_{PC\text{-}HET}$ and $k_{PC\text{-}AOB}$ were 0.000180 ± 0.000017 and 0.000140 ± 0.000012 m^3 g COD^{-1} h^{-1}, which were lower than but in the same order of magnitude as the literature reported values (0.00093 ± 0.00018 and 0.00067 ± 0.00023 m^3 g COD^{-1} h^{-1}, respectively).[20] The discrepancy in these parameters values could be probably ascribed to the difference in the community structure in the adopted nitrifying cultures or different operating conditions. The model could be potentially applied to a widespread extent despite that the parameter values would vary according to the experimental conditions. As suggested, it was difficult to compare these coefficients ($k_{PC\text{-}HET}$, $k_{PC\text{-}AOB}$ and $T^{c}_{PC\text{-}AOB}$) with other pharmaceuticals as most existing models did not consider the specific biochemical processes.[20]

Model validation with atenolol biotransformation under different conditions

In order to further confirm the validity and reliability of the developed model, model validation was carried out to compare the model simulations to the independent experimental data, which were not used for model calibration. Based on the measured concentrations of atenolol and atenolol acid, the stoichiometric coefficients α^{c}_{BP} and α^{m}_{BP} were calculated as 0.58 and 0.58, respectively. Applied with previously calibrated parameters in Table 1, the

proposed biotransformation model was used to predict dynamics of ammonium, nitrite, DO, atenolol and atenolol acid in the presence of ammonium at a constant concentration of 25 mg-N L^{-1} and at DO of around 2.5 mg L^{-1} (significantly different from the ammonium of 50 mg-N L^{-1} and DO of 3.0 mg L^{-1} used for model calibration). The model captured the dynamics of ammonium, nitrite and DO, again suggesting the validity of the two-step nitrification model and the suitability of the selected parameters related to DO (see Figure S2B). As shown in Figure 2, atenolol continuously dropped from initial 15 μg L^{-1} with a final degradation efficiency of 92.9%. The conversion rate of atenolol acid transformed from atenolol was calculated as 57.9%. The model predictions could capture these trends of atenolol degradation and atenolol acid formation very well, which again supports the validity of the developed model for atenolol biotransformation.

Model evaluation with experimental data from acyclovir biotransformation

The experimental results obtained with Case *II* for biotransformation of acyclovir were used to further evaluate the developed model. The developed biotransformation model was recalibrated for acyclovir biodegradation and carboxy-acyclovir formation dynamics under different conditions. Most of the literature reported model parameters were employed at same values as the case of atenolol except the stoichiometry coefficients (α^m_{BP}, α^c_{BP}, β^m_{BP}, β^c_{BP}) for formation of carboxy-acyclovir associated with specific biochemical processes (as shown in Table S4 in SI), which were calculated based on the experimental data. The values for the three key parameters $k_{PC\text{-}HET}$, $k_{PC\text{-}AOB}$ and $T^c_{PC\text{-}AOB}$ were recalibrated, which were associated with the investigated parent compound. As the enriched nitrifying biomass utilized in the batch biodegradation experiments of acyclovir were same as those in case of atenolol, the maximum growth rate of AOB $\mu_{max,\ AOB}$ was set to be the same as in case of atenolol during model calibration for acyclovir biotransformation in the presence of ammonium. The

obtained parameter values for acyclovir biotransformation were 0.00035 ± 0.00002 m^3 g COD^{-1} h^{-1} ($k_{PC\text{-}HET}$), 0.00005 ± 0.00003 m^3 g COD^{-1} h^{-1} ($k_{PC\text{-}AOB}$) and 0.00093 ± 0.00049 m^3 g COD^{-1} ($T^c_{PC\text{-}AOB}$).

The model predictions of acyclovir biotransformation matched the experimental results well under different conditions (Figure 3), further demonstrating the validity of the established model. Parameters values giving the optimum fits with the experimental data were difficult to compare reliably with literature values as this study firstly reported the AOB cometabolic acyclovir transform coefficient $T^c_{PC\text{-}AOB}$. However, compared to other reported compounds, e.g. atenolol,[20] it was obvious that parameters $k_{PC\text{-}AOB}$ and $T^c_{PC\text{-}AOB}$ for acyclovir were lower than those values for atenolol (Table 1), indicating a stronger degradation ability of the AOB culture studied on atenolol than acyclovir. Considering the molecular differences between these two pharmaceuticals, this may imply an affinity property of AOB for different compounds probably due to a preferential substrate selection to AMO active sites.[31] The parameter $k_{PC\text{-}HET}$ for acyclovir was 0.00035 ± 0.00002 m^3 g COD^{-1} h^{-1}, which was in the same order of magnitude of the value estimated in this study (0.000180 ± 0.000017 m^3 g COD^{-1} h^{-1}) for atenolol. The conversion efficiencies from acyclovir to carboxy-acyclovir were 83.9%, 43.0% and 29.9% in Experiments 1, 2 and 3, respectively (see Figure 3). These results indicated the importance of metabolism of acyclovir by HET. Oxidation of acyclovir to carboxy-acyclovir might be dominated by unspecific monoxygenase from HET,[32] which needs to be confirmed in the further work.

Discussion

In this work, a comprehensive mathematical model is developed to describe the biotransformation of pharmaceuticals and the formation of their products by enriched nitrifying cultures. In the proposed model, processes 1 and 2 (Table S2 in SI) depict the

AOB-induced cometabolic and metabolic biotransformation of pharmaceuticals, while processes 5 and 6 (Table S2 in SI) describe the HET-induced cometabolic and metabolic biotransformation of pharmaceuticals, respectively. Sensitivity analysis indicated that four key parameters $k_{PC\text{-}HET}$, $k_{PC\text{-}AOB}$, $T^{c}_{PC\text{-}AOB}$and $\mu_{max,\ AOB}$ were critical to the model output and therefore estimated through model calibration. The validity of this biotransformation model is confirmed by independent atenolol biodegradation data and further evaluated by acyclovir biotransformation experiments. Compared to the previous studies where atenolol biodegradation was investigated through experiments and modeling approaches,[20,21] the proposed model in this work considers the formation of biotransformation products and describes biotransformation of different pharmaceuticals under different metabolic conditions. This microbial processes-linked biotransformation model could enhance our ability to predict the fate of pharmaceuticals and their transformation products during wastewater treatment processes.

Since we estimated four model parameters for fitting the experimental data, parameter uniqueness is important, since it is possible that different parameter combinations can give similar simulation accuracy. In our work, we applied a least-squared analysis and evaluated standard errors and 95% confidence intervals of individual parameter estimates. The parameter confidence intervals showed a well-defined range in which the optimum values of parameters reside (Table 1), which indicates good uniqueness of these parameters. In addition to the analysis of the confidence intervals, two other aspects of our experimental design support the uniqueness of the parameter values. First, we used five different experimental parameters (ammonium, nitrite, DO, parent compound, and biotransformation product), which reflect different aspects of the kinetics of the two-step nitrification and pharmaceutical biotransformation by enriched nitrifying culture. Second, we carried out independent experiments to validate the estimated parameters. In particular, the good correspondence for

independent experimental data supports the validity of the new model and the uniqueness of the parameters for pharmaceutical biotransformation.

The modeling results in this work suggested the cometabolism induced by AOB could play an important role in the pharmaceutical removal in the studied ratio ranges of pharmaceuticals to ammonia for cometabolism. Indeed a positive linear relationship was observed between ammonia oxidation rate and pharmaceutical degradation rates in terms of atenolol and acyclovir based on the validated model (Figure 4A). The atenolol degradation rate increased from 0.012 to 0.16 μg g VSS^{-1} h^{-1} while the nitrification rate increased from 2.84 to 59.15 mg NH_4^+-N g VSS^{-1} h^{-1}. With respect to acyclovir, the degradation rate changed from 0.014 to 0.10 μg g VSS^{-1} h^{-1} whereas the ammonia oxidation rate showed an increase from 2.37 to 36.63 mg NH_4^+-N g VSS^{-1} h^{-1}. Such a positive correlation was also reported in previous literature under certain conditions,[7,22,25] supporting the notion that majority of atenolol and acyclovir could be cometabolically degraded in the enriched nitrifying cultures. A further assessment on the wide application of the relationship was carried out by simulating the concentration profiles of pharmaceuticals after 240 h. The molar ratios of atenolol to ammonia from 8.42×10^{-7} to 1.91×10^{-5} calculated based on their concentrations was observed to be still within the range for a linearly positive relationship regarding the cometabolic biodegradation of atenolol by the enriched nitrifying cultures used in this work, and the relationship maintained at a same slope (Black solid squares in Figure 4A demonstrated the predicted atenolol degradation rate after 240 h). However, a different slope was found for the relationship between ammonia oxidation rate and the acyclovir degradation rate after 240 h predicted using the developed model (Figure 4B). If the ammonia oxidation rate was higher than the critical value (2.3 mg NH_4^+-N g VSS^{-1} h^{-1} in this study), the lower slope might indicate a slower increasing trend in acyclovir degradation rate with an increasing ammonia oxidation rate (Figure 4A). Compared with the situation at the lower

ammonia oxidation rate, a higher increasing trend in acyclovir degradation rate would arise at higher slope (Figure 4B). The observation that pharmaceutical would not be degraded until the ammonia was depleted[33] revealed a higher pharmaceutical degradation rate at lower ammonia oxidation rate, which supported the findings in this study. Regardless of the different slopes for the relationship, the molar ratios of acyclovir to ammonia ranging from 1.62×10^{-11} to 2.26×10^{-5} was obtained to be a valid application range for the cometabolic biodegradation of acyclovir by the enriched nitrifying cultures used in this work.

The proposed model framework was expected to be a useful tool to predict the biotransformation of pharmaceuticals and the formation of transformation products under varying conditions, therefore providing the guidance in designing, upgrading and optimizing of the relevant biological wastewater treatment processes. The influence of DO on pharmaceutical biotransformation was investigated by performing model simulations in the enriched nitrifying systems. The pharmaceutical removal efficiencies at 240 h at different DO concentrations ranging from 0 to 4 mg L^{-1} with ammonium concentration of 50 mg-N L^{-1} are shown in Figure 5. Overall DO concentration had a positive effect on pharmaceutical removal efficiencies. The concentrations of atenolol and acyclovir decreased rapidly with a prompt increase of atenolol acid and carboxy-acyclovir as DO increased to 1 mg L^{-1}. With DO further increased to 4 mg L^{-1}, a gradual decrease of pharmaceutical concentrations was observed accompanied with a slight increase of their biotransformation products. The degradation efficiencies for atenolol at DO concentrations of 0, 1 and 4 mg L^{-1} were 44.3%, 83.2% and 94.0%, respectively. With regard to acyclovir, its degradation efficiencies were observed to be 36.2%, 81.2% and 87.3%, respectively at DO of 0, 1 and 4 mg L^{-1}. The simulation results revealed that the DO concentration would play an important role in pharmaceutical biotransformation. This was contrary to the previous report that DO in the WWTP had no influence on oxidative biotransformation of selected micropollutants.[34] The

415 possible reason could be that the experiments conducted in this study were nitrifying culture
416 based instead of the regular activated sludge in WWTP, suggesting that DO might regulate
417 the pharmaceutical biotransformation cometabolically. It should be noted that the simulation
418 results are to provide insight into the potential impact of DO on pharmaceutical
419 biotransformation by enriched nitrifying culture rather than to accurately predict the reality,
420 which remain to be verified in future work.

421 The growth substrate might also have an impact on the pharmaceutical biotransformation.
422 Different ammonium concentrations ranging from 0 to 100 mg L^{-1} were applied in the model
423 simulations at different DO concentrations as shown in Figure 6. It was obvious that the
424 degradation efficiencies of studied pharmaceuticals and the formation rates of their
425 transformation products would increase dramatically when ammonium concentrations
426 increase from 0 to 20 mg-N L^{-1}, especially in case of atenolol suggesting the importance of
427 cometabolism on its biotransformation. However, there was no significant enhancement with
428 the increase of ammonium concentrations from 20 to 250 mg-N L^{-1} (data of 100-250 mg-N L^{-1}
429 were not shown). This was contrary to the previous report where the removal efficiencies of
430 the selected pharmaceuticals were enhanced at higher initial ammonium concentrations.[35]
431 This could be probably due to the substrate competition between growth substrate
432 (ammonium) and cometabolic substrates (e.g. atenolol or acyclovir). Pharmaceutical levels
433 applied in this study were several orders of magnitude lower than the investigated ammonium
434 concentrations, leading to a competition for AMO active sites and therefore potential
435 decreasing degradation rates at higher ammonium concentrations.[31,33]

436 In summary, a comprehensive model that considers all microbial processes contributing
437 to pharmaceutical biotransformation as well as the formation of biotransformation products
438 by the enriched nitrifying cultures is developed in this work. The proposed model was
439 successfully calibrated and validated using the biotransformation experiments of atenolol and

acyclovir under different metabolic conditions. The linear positive correlation between ammonia oxidation rate and pharmaceutical degradation rate confirmed the major role of cometabolism induced by AOB in the pharmaceutical removal. DO was revealed to be capable of regulating the pharmaceutical biotransformation cometabolically and the substrate competition between ammonium and pharmaceuticals existed at high ammonium concentrations. More verification should be conducted using other pharmaceuticals' biotransformation data for this developed model to facilitate its application as a useful tool in prediction of pharmaceutical fate, especially in the real municipal wastewater systems, where other processes (e.g., the competition between different parent compounds on the enzyme active sites) need to be considered in future work.

Acknowledgement

This study was supported by the Australian Research Council (ARC) through Future Fellowship FT160100195. Dr. Bing-Jie Ni acknowledges the support of ARC Discovery Project DP130103147.

Supporting Information

Additional texts, tables and figures are shown in Supporting Information.

Reference

(1) Ternes, T. A., Occurrence of drugs in German sewage treatment plants and rivers. *Water Res.* **1998,** *32* (11), 3245-3260.

(2) Benner, J.; Helbling, D. E.; Kohler, H. P. E.; Wittebol, J.; Kaiser, E.; Prasse, C.; Ternes, T. A.; Albers, C. N.; Aamand, J.; Horemans, B.; Springael, D.; Walravens, E.; Boon, N., Is biological treatment a viable alternative for micropollutant removal in drinking water treatment processes? *Water Res.* **2013,** *47* (16), 5955-5976.

(3) Petrie, B.; Barden, R.; Kasprzyk-Hordern, B., A review on emerging contaminants in wastewaters and the environment: Current knowledge, understudied areas and recommendations for future monitoring. *Water Res.* **2015,** *72*, 3-27.

(4) Evgenidou, E. N.; Konstantinou, I. K.; Lambropoulou, D. A., Occurrence and removal of transformation products of PPCPs and illicit drugs in wastewaters: A review. *Sci. Total Environ.* **2015,** *505*, 905-926.

(5) Carballa, M.; Omil, F.; Lema, J. M.; Llompart, M. a.; García-Jares, C.; Rodríguez, I.; Gómez, M.; Ternes, T., Behavior of pharmaceuticals, cosmetics and hormones in a sewage treatment plant. *Water Res.* **2004,** *38*, (12), 2918-2926.

(6) Batt, A. L.; Kim, S.; Aga, D. S., Enhanced biodegradation of iopromide and trimethoprim in nitrifying activated sludge. *Environ. Sci. Technol.* **2006,** *40* (23), 7367-7373.

(7) Yi, T.; Harper Jr, W. F., The link between nitrification and biotransformation of 17α-ethinylestradiol. *Environ. Sci. Technol.* **2007,** *41* (12), 4311-4316.

(8) Keener, W. K.; Arp, D. J., Kinetic studies of ammonia monooxygenase inhibition in Nitrosomonas europaea by hydrocarbons and halogenated hydrocarbons in an optimized whole- cell assay. *Appl. Environ. Microbiol.* **1993,** *59* (8), 2501-2510.

(9) Keener, W. K.; Arp, D. J., Transformations of aromatic compounds by Nitrosomonas europaea. *Appl. Environ. Microbiol.* **1994,** *60* (6), 1914-1920.

(10) Xu, Y.; Yuan, Z.; Ni, B.-J., Biotransformation of pharmaceuticals by ammonia oxidizing bacteria in wastewater treatment processes. *Sci. Total Environ.* **2016,** *566–567*, 796-805.

(11) Tran, N. H.; Urase, T.; Ngo, H. H.; Hu, J.; Ong, S. L., Insight into metabolic and cometabolic activities of autotrophic and heterotrophic microorganisms in the biodegradation of emerging trace organic contaminants. *Bioresour. Technol.* **2013,** *146*, (0), 721-731.

(12) Quintana, J. B.; Weiss, S.; Reemtsma, T., Pathways and metabolites of microbial degradation of selected acidic pharmaceutical and their occurrence in municipal wastewater treated by a membrane bioreactor. *Water Res.* **2005,** *39* (12), 2654-2664.

(13) Fernandez-Fontaina, E.; Carballa, M.; Omil, F.; Lema, J. M., Modelling cometabolic biotransformation of organic micropollutants in nitrifying reactors. *Water Res.* **2014,** *65*, 371-383.

(14) Oldenhuis, R.; Vink, R. L. J. M.; Janssen, D. B.; Witholt, B., Degradation of chlorinated aliphatic hydrocarbons by Methylosinus trichosporium OB3b expressing soluble methane monooxygenase. *Appl. Environ. Microbiol.* **1989,** *55* (11), 2819-2826.

(15) Liu, L.; Binning, P. J.; Smets, B. F., Evaluating alternate biokinetic models for trace pollutant cometabolism. *Environ. Sci. Technol.* **2015,** *49* (4), 2230-2236.

(16) Verlicchi, P.; Al Aukidy, M.; Zambello, E., Occurrence of pharmaceutical compounds in urban wastewater: Removal, mass load and environmental risk after a secondary treatment—A review. *Sci. Total Environ.* **2012,** *429*, 123-155.

(17) Prasse, C.; Schlüsener, M. P.; Schulz, R.; Ternes, T. A., Antiviral drugs in wastewater and surface waters: a new pharmaceutical class of environmental relevance? *Environ. Sci. Technol.* **2010,** *44* (5), 1728-1735.

(18) Prasse, C.; Wagner, M.; Schulz, R.; Ternes, T. A., Biotransformation of the antiviral drugs acyclovir and penciclovir in activated sludge treatment. *Environ. Sci. Technol.* **2011,** *45* (7), 2761-2769.

(19) Radjenović, J.; Pérez, S.; Petrović, M.; Barceló, D., Identification and structural characterization of biodegradation products of atenolol and glibenclamide by liquid chromatography coupled to hybrid quadrupole time-of-flight and quadrupole ion trap mass spectrometry. *J. Chromatogr. A* **2008,** *1210* (2), 142-153.

(20) Sathyamoorthy, S.; Chandran, K.; Ramsburg, C. A., Biodegradation and cometabolic modeling of selected beta blockers during ammonia oxidation. *Environ. Sci. Technol.* **2013,** *47* (22), 12835-12843.

(21) Xu, Y.; Yuan, Z.; Ni, B.-J., Impact of Ammonium Availability on Atenolol Biotransformation during Nitrification. *ACS Sustainable Chem. Eng.* **2017,** *5* (8), 7137-7144.

(22) Xu, Y.; Yuan, Z.; Ni, B.-J., Biotransformation of acyclovir by an enriched nitrifying culture. *Chemosphere* **2017,** *170*, 25-32.

(23) Ginestet, P.; Audic, J. M.; Urbain, V.; Block, J. C., Estimation of nitrifying bacterial activities by measuring oxygen uptake in the presence of the metabolic inhibitors allylthiourea and azide. *Appl. Environ. Microbiol.* **1998,** *64* (6), 2266-2268.

(24) Ali, T. U.; Kim, M.; Kim, D. J., Selective inhibition of ammonia oxidation and nitrite oxidation linked to n2o emission with activated sludge and enriched nitrifiers. *J. Microbiol. Biotechnol.* **2013,** *23* (5), 719-723.

(25) Xu, Y.; Radjenovic, J.; Yuan, Z.; Ni, B. J., Biodegradation of atenolol by an enriched nitrifying sludge: Products and pathways. *Chem. Eng. J.* **2017,** *312*, 351-359.

(26) Kasim, N. A.; Whitehouse, M.; Ramachandran, C.; Bermejo, M.; Lennernäs, H.; Hussain, A. S.; Junginger, H. E.; Stavchansky, S. A.; Midha, K. K.; Shah, V. P.; Amidon, G. L., Molecular properties of WHO essential drugs and provisional biopharmaceutical classification. *Mol. Pharmaceutics* **2004,** *1* (1), 85-96.

(27) Maurer, M.; Escher, B. I.; Richle, P.; Schaffner, C.; Alder, A. C., Elimination of β-blockers in sewage treatment plants. *Water Res.* **2007,** *41* (7), 1614-1622.

(28) Mohsen-Nia, M.; Ebrahimabadi, A. H.; Niknahad, B., Partition coefficient n-octanol/water of propranolol and atenolol at different temperatures: Experimental and theoretical studies. *J. Chem. Thermodyn.* **2012,** *54*, 393-397.

(29) Küster, A.; Alder, A. C.; Escher, B. I.; Duis, K.; Fenner, K.; Garric, J.; Hutchinson, T. H.; Lapen, D. R.; Péry, A.; Römbke, J.; Snape, J.; Ternes, T.; Topp, E.; Wehrhan, A.; Knackerk, T., Environmental risk assessment of human pharmaceuticals in the European union: A case study with the β-blocker atenolol. *Integr. Environ. Assess. Manage.* **2010,** *6* (SUPPL. 1), 514-523.

(30) Batstone, D. J.; Pind, P. F.; Angelidaki, I., Kinetics of thermophilic anaerobic oxidation of straight and branched chain butyrate and valerate. *Biotechnol. Bioeng.* **2003**, *84* (2), 195-204.

(31) Fernandez-Fontaina, E.; Omil, F.; Lema, J. M.; Carballa, M., Influence of nitrifying conditions on the biodegradation and sorption of emerging micropollutants. *Water Res.* **2012,** *46* (16), 5434-5444.

(32) Men, Y.; Han, P.; Helbling, D. E.; Jehmlich, N.; Herbold, C.; Gulde, R.; Onnis-Hayden, A.; Gu, A. Z.; Johnson, D. R.; Wagner, M.; Fenner, K., Biotransformation of Two Pharmaceuticals by the Ammonia-Oxidizing Archaeon *Nitrososphaera gargensis*. *Environ. Sci. Technol.* **2016,** *50* (9), 4682-4692.

(33) Dawas-Massalha, A.; Gur-Reznik, S.; Lerman, S.; Sabbah, I.; Dosoretz, C. G., Co-metabolic oxidation of pharmaceutical compounds by a nitrifying bacterial enrichment. *Bioresour. Technol.* **2014,** *167*, 336-342.

(34) Helbling, D. E.; Johnson, D. R.; Honti, M.; Fenner, K., Micropollutant biotransformation kinetics associate with WWTP process parameters and microbial community characteristics. *Environ. Sci. Technol.* **2012,** *46* (19), 10579-10588.

(35) Tran, N. H.; Urase, T.; Kusakabe, O., The characteristics of enriched nitrifier culture in the degradation of selected pharmaceutically active compounds. *J. Hazard. Mater.* **2009,** *171* (1–3), 1051-1057.

Table and Figure Legends

Table 1. Estimated parameter values for the biotransformation model in this study

Figure 1. Model calibration with experimental data from atenolol biodegradation: (A) Experiment 1, with addition of allylthiourea (ATU); (B) Experiment 2, in the absence of ammonium; and (C) Experiment 3, in the presence of ammonium (50 mg NH_4^+-N L^{-1}).

Figure 2. Model validation results of atenolol biotransformation by the enriched nitrifying culture in the presence of ammonium of 25 mg-N L^{-1} (Experiment 4).

Figure 3. Model evaluation with experimental data from acyclovir biodegradation: (A) Experiment 1, with addition of allylthiourea (ATU), (B) Experiment 2, in the absence of ammonium and (C) Experiment 3, in the presence of ammonium (50 mg NH_4^+-N L^{-1}).

Figure 4. (A) The relationship between ammonia oxidizing rate and the pharmaceutical degradation rates in terms of atenolol and acyclovir (black solid squares indicate the atenolol degradation rates after 240 h); and (B) The relationship between ammonia oxidizing rate and the acyclovir degradation rate after 240 h at a different linear fit slope.

Figure 5. Predicted final concentrations of (A) atenolol and atenolol acid and (B) acyclovir and carboxy-acyclovir at time of 240 h at different concentrations of dissolved oxygen (DO) in the enriched nitrifying culture system.

Figure 6. Predicted concentrations of pharmaceuticals and their transformation products at time of 240 h at initial concentrations of 15 μg L^{-1} with different ammonium concentrations ranging from 0 to 100 mg-N L^{-1} at different DO levels.

593 **Table 1.** Estimated parameter values for the biotransformation model in this study

Parameters	Definition	Unit	Estimated	
			atenolol	acyclovir
$k_{PC\text{-}HET}$	Heterotrophs (HET) transformation coefficient	m^3 g COD^{-1} h^{-1}	0.000180 ± 0.000017	0.00035 ± 0.00002
$k_{PC\text{-}AOB}$	Ammonia oxidizing bacteria (AOB) transformation coefficient	m^3 g COD^{-1} h^{-1}	0.000140 ± 0.000012	0.00005 ± 0.00003
$T^{c}_{PC\text{-}AOB}$	Parent compound biotransformation coefficient rate linked to AOB growth (cometabolism)	m^3 g COD^{-1}	0.012 ± 0.000036	0.00093 ± 0.00049
$\mu_{max,\ AOB}$	Maximum specific growth rate of AOB	h^{-1}	0.012 ± 0.0023	

594

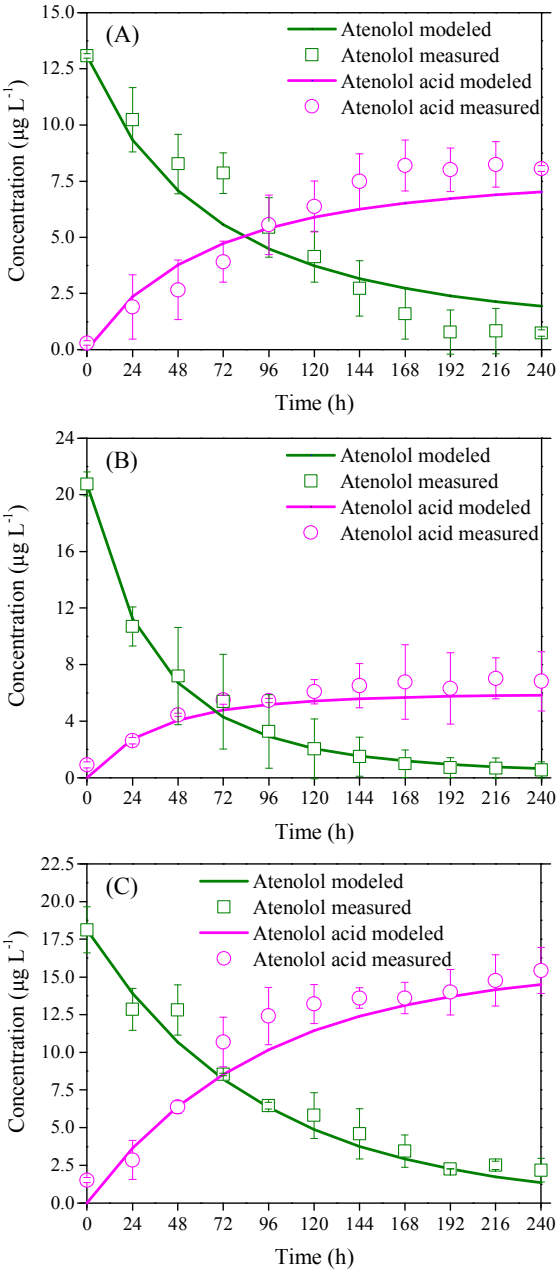

595

596 **Figure 1.** Model calibration with experimental data from atenolol biodegradation: (A)
597 Experiment 1, with addition of allylthiourea (ATU); (B) Experiment 2, in the absence of
598 ammonium; and (C) Experiment 3, in the presence of ammonium (50 mg NH_4^+-N L^{-1}).

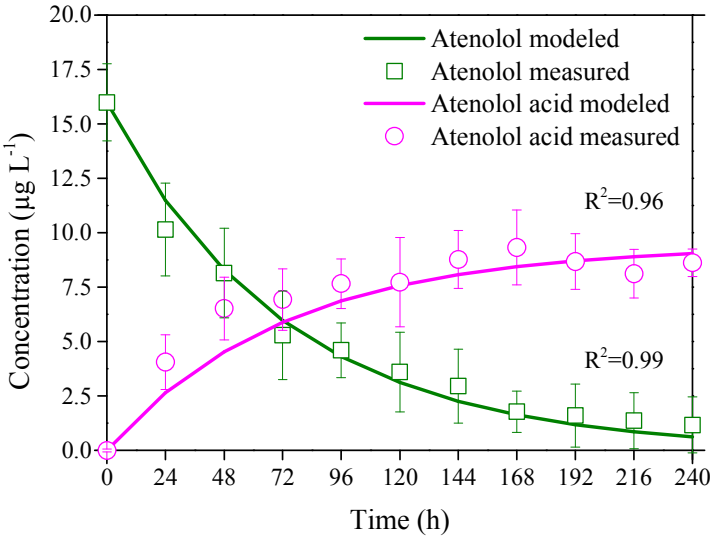

599

600

601 **Figure 2.** Model validation results of atenolol biotransformation by the enriched nitrifying

602 culture in the presence of ammonium of 25 mg-N L^{-1} (Experiment 4).

603

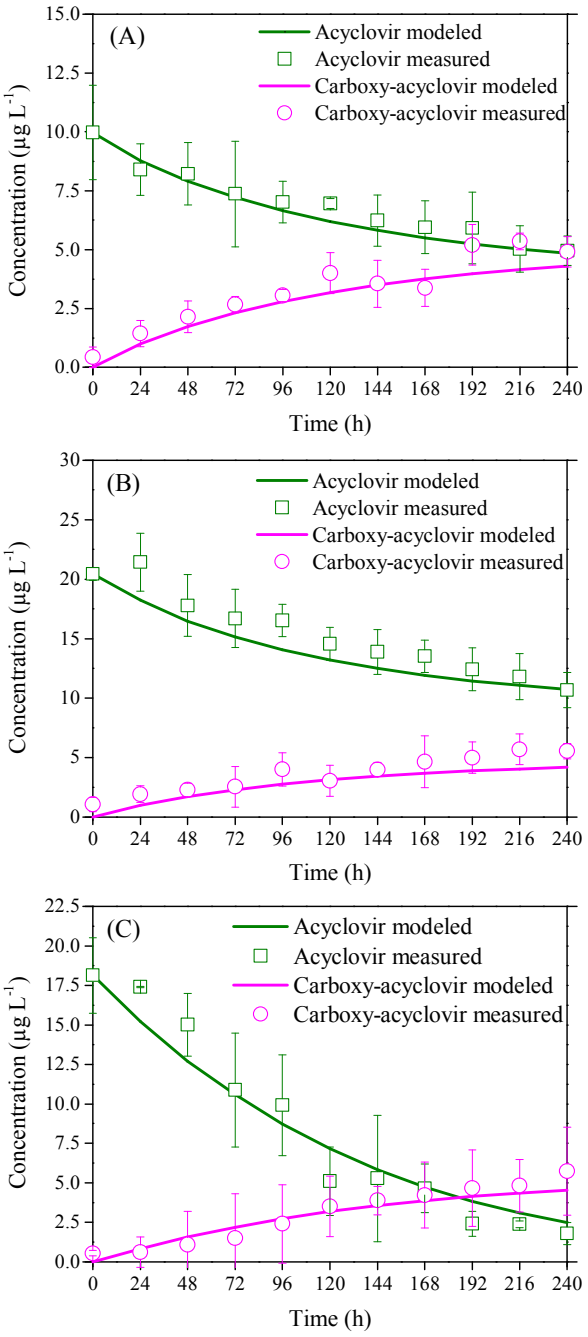

Figure 3. Model evaluation with experimental data from acyclovir biodegradation: (A) Experiment 1, with addition of allylthiourea (ATU), (B) Experiment 2, in the absence of ammonium and (C) Experiment 3, in the presence of ammonium (50 mg NH_4^+-N L^{-1}).

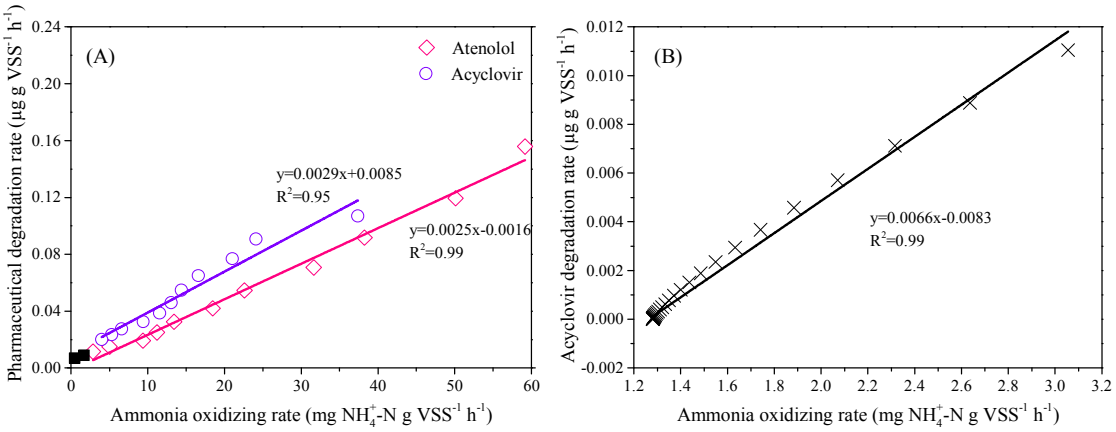

Figure 4. (A) The relationship between ammonia oxidizing rate and the pharmaceutical degradation rates in terms of atenolol and acyclovir (black solid squares indicate the atenolol degradation rates after 240 h); and (B) The relationship between ammonia oxidizing rate and the acyclovir degradation rate after 240 h at a different linear fit slope.

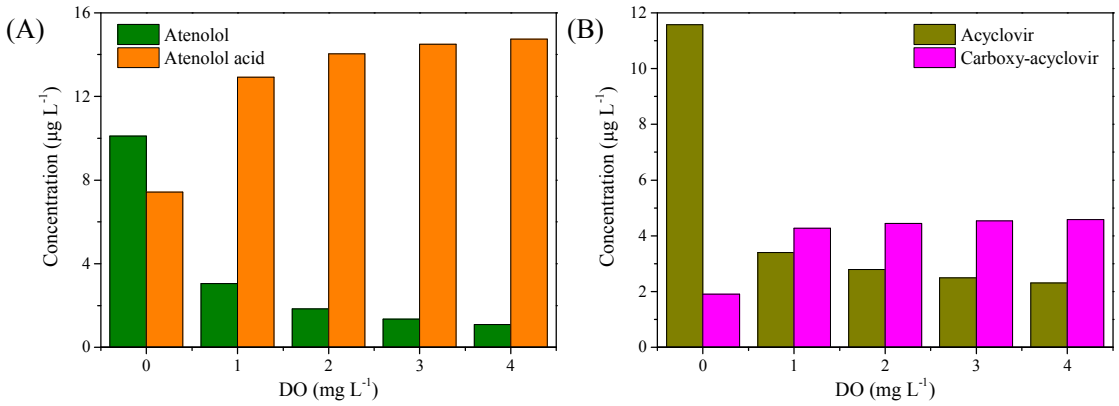

614

615 **Figure 5.** Predicted final concentrations of (A) atenolol and atenolol acid and (B) acyclovir
616 and carboxy-acyclovir at time of 240 h at different concentrations of dissolved oxygen (DO)
617 in the enriched nitrifying culture system.

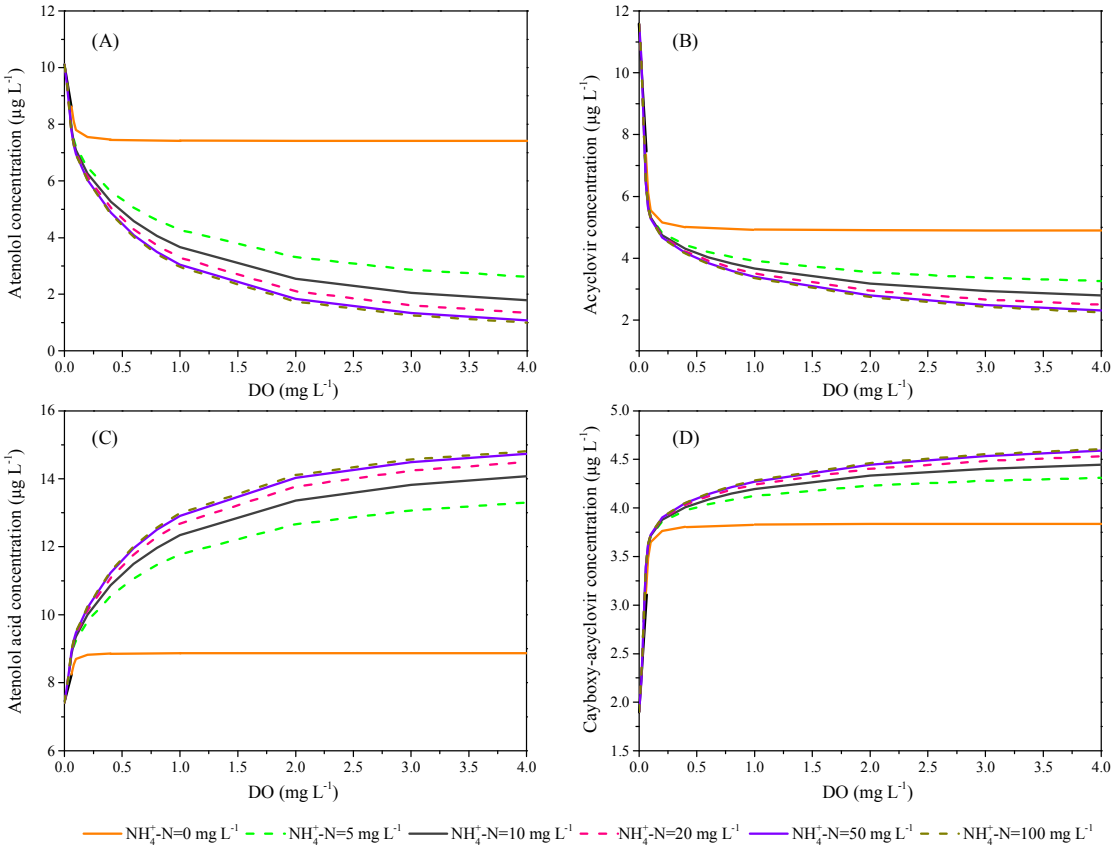

618

619 **Figure 6.** Predicted concentrations of pharmaceuticals and their transformation products at
620 time of 240 h at initial concentrations of 15 μg L^{-1} with different ammonium concentrations
621 ranging from 0 to 100 mg-N L^{-1} at different DO levels.